Open access • Journal Article • DOI:10.1039/C4NR07233B

A tunable submicro-optofluidic polymer filter based on guided-mode resonance.

Guohui Xiao, Qiangzhong Zhu, Yang Shen, Kezheng Li ...+3 more authors

Institutions: Sun Yat-sen University, Australian National University, Lancaster University

Published on: 12 Feb 2015 - Nanoscale (Nanoscale)

Topics: Optical filter, Waveguide filter, Guided-mode resonance, Waveguide (optics) and Filter (video)

Nanoscale

Accepted Manuscript

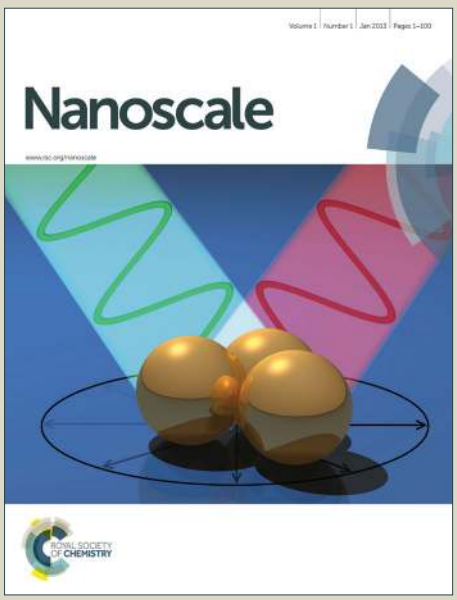

ROYAL SOCIETY OF CHEMISTRY

www.rsc.org/nanoscale

Cite this: DOI: 10.1039/c0xx00000x

www.rsc.org/xxxxxx

COMMUNICATION

A tunable submicro-optofluidic polymer filter based on guided-mode resonance

Guohui Xiao[a], Qiangzhong Zhu[a], Yang Shen[a], Kezheng Li[a], Mingkai Liu[b], Qiandong Zhuang[c] and Chongjun Jin*[a]

Received (in XXX, XXX) Xth XXXXXXXXX 20XX, Accepted Xth XXXXXXXXX 20XX
DOI: 10.1039/b000000x

Optical filters with reconfigurable spectral properties are highly desirable in a wide range of applications. We propose and experimentally demonstrate a tunable submicro-optofluidic polymer guided-mode resonance (PGMR) filter. The device is composed of a periodic grating sandwiched between a high index waveguide layer and a low index capping layer, which integrates submicro-fluidic channel arrays and PGMR filter elegantly. A finite difference time domain (FDTD) methods is employed to understand the spectral properties and determine appropriate device parameters. We fabricate the polymer guided-mode resonance filter with a method combining two-beam interference lithography, floating nanofilm transfer and thermal bonding techniques. Experimental results show that our tunable submicro-optofluidic PGMR filters can provide a broad spectral tuning range (13.181 nm), a narrow bandwidth (< 2.504 nm), and a high reflection efficiency (> 85%) in the visible region. Such submicro-optofluidic PGMR filters are highly compatible with existing nano/microfluidic technologies and would be valuable for the integrated flexible optical system.

Guided-mode resonance (GMR) filters associated with diffraction anomaly[1,2] of periodic surface structures represent a unique class of narrow-band filters with almost 100% reflection efficiency. Up to now, a large number of devices based on GMR, such as optical switchers,[3] light modulators,[4,5] and filters[6,7] have been demonstrated, and they are widely used in communication,[8] display,[9,10] and bio-sensing.[11-13] However, due to fabrication errors, the GMR filters do not always work on their designed spectral position, and reconfigurable devices are of particular interest. Recently, some tunable GMR filters have been experimentally demonstrated, in which various tuning mechanisms, including electro-optic effects,[14-16] thermo-optic effects,[17] optically induced trans-cis isomerization of azobenzene liquid crystals,[18,19] MEMS,[20] and variation of incident angle,[21] were exploited.

Compared with the materials used in the above tunable GMR filters, polymers provide an attractive alternative for GMR filter due to their diverse range of physiochemical properties, low material cost, and simple fabrication techniques. Moreover, polymers are widely used in microfluidic devices,[22,23] and it is possible to realize a tunable polymer GMR (PGMR) device based on nano/microfluidic methods.

Optofluidics is defined as the fusion of optics and nano/microfluidics,[24] which represents a unique approach for fluid manipulating light and light manipulating fluid. Optofluidic devices exhibit unique tunability since fluids (liquids or gases) provide a wide choice of compositions. Building on these merits of optofluidic techniques, a lot of flexible optofluidic devices have been developed, such as tunable optical filter,[25-27] tunable light switches,[28,29] tunable dye laser,[30] tunable microlens,[31,32] tunable attenuators,[33] tunable Michelson interferometer,[34] sensor.[35,36] It is therefore expected that the combination of polymer submicro-fluidic channels and guided-mode resonance filter can be a feasible method for fine tuning the filter response. As far as our knowledge concerns, a tunable PGMR filter in the visible light region based on nano/microfluidic methods has not been reported.

In this paper, we present a novel tunable optofluidic polymer guided-mode resonance (PGMR) filter based on submicro-channels. The submicro-channel arrays were fabricated with a simple and cost-effective polymer-based technique, and the optical property of the filter can be tuned by the fluidic mixture in the channels. A finite difference time domain (FDTD) method was used to understand the optical property of the device and design the optimal structural parameters. Our tunable submicro-optofluidic PGMR filter is featured with a high reflection efficiency and broad tuning range in the visible wavelength. Importantly, our polymer-based device is highly compatible with existing nano/microfluidic technologies and it would be a favorable solution for miniaturized optical detection systems on a nano/microfluidic platform.

The configuration of the tunable submicro-optofluidic PGMR filter is illustrated in Fig. 1(a). The device consists of a square-wave profile photoresist (n_H = 1.61) grating layer, sandwiched between two homogeneous polymer films on the quartz substrate. A thermoplastic polymer of poly(methyl methacrylate) (PMMA) with a refractive index (n_{cap} = 1.49) is used as the capping layer, which is essential to form the sealed single-layered submicro-channels (as will be discussed in Fabrication). While poly(9-vinylcarbazole) (PVK) with a high refractive index (n_w = 1.69) is functioned as a waveguide layer and bottom cladding. The refractive indices of the environment and substrate are set as n_c = 1.0, and n_s = 1.46, respectively. The structural parameters of the

Cite this: DOI: 10.1039/c0xx00000x

www.rsc.org/xxxxxx

COMMUNICATION

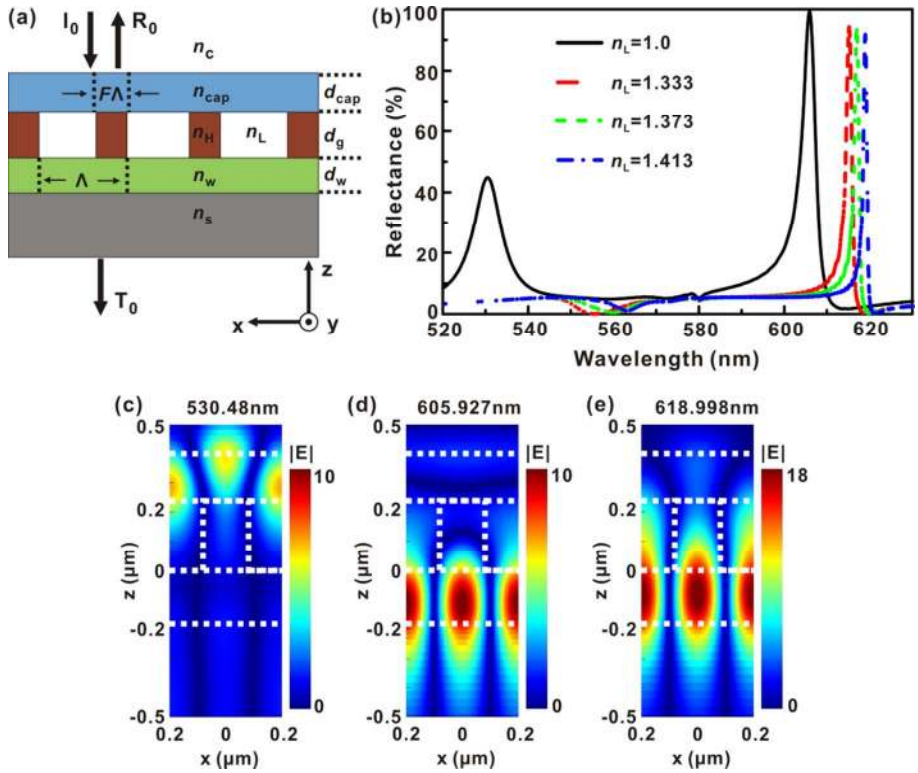

Fig. 1 (a) Scheme of the PGMR filter with a single-layer submicro-channels. (b) Simulated reflectance spectra of the PGMR filter when the channels were filled with different solutions, where d_{cap} = 200 nm, d_g = 240 nm, d_w = 180 nm, n_c = 1.0, n_{cap} = 1.49, n_H = 1.61, n_w =1.69, n_s = 1.46, F = 0.4, and Λ = 400 nm. (c) The distribution of electric field amplitude at the resonance wavelength of 530.48 nm when n_L = 1.0; (d and e) The distributions of electric field amplitudes at the resonance wavelength of 605.927 nm and 618.998 nm when n_L = 1.0 and 1.413 respectively. The incident wave is TE polarized plane wave. The white dashed lines are structural outlines, and only one unit cell is illustrated.

device, d_{cap}, d_g, d_w, and Λ are the thickness of PMMA layer, grating layer, PVK layer, and the period of the grating, respectively. The filling factor (F) is defined as the ratio of the grating ridge to the period.

According to the effective media theory, the effective index of the grating layer for TE-polarized incident plane wave (electric field parallel to the ridges of the grating) can be estimated by[37]

$$n_{\text{eff}} = \left[F n_{\text{H}}^2 + (1-F) n_{\text{L}}^2 \right]^{1/2}, \quad (1)$$

where n_H and n_L represent the refractive indices of photoresist and air, respectively. Guided-mode resonance occurs when the incident wave is coupled with a guided-mode supported by the multilayered structure under phase matching conditions. When the dissipation loss is negligible, the regime of different orders of resonance can be estimated by the inequality,[38]

$$\max\{n_c, n_s\} \le \left| \frac{j\lambda}{\Lambda} \right| \le \max\{n_{cap}, n_{eff}, n_w\}, \quad (j = \pm 1, \pm 2, \pm 3,...). \quad (2)$$

where j is the order of diffracted evanescent-waves propagating in the waveguide layer, and λ is the resonant wavelength. To obtain highly efficient filters (typical for $j = \pm 1$), the period of the grating needs to be sufficiently smaller than the target resonance wavelength ($\Lambda < \lambda$), such that only the zeroth order wave propagates.

The optical responses of the PGMR filter is simulated with the finite difference time domain (FDTD) method (Lumerical FDTD solutions). By employing the optimization method,[39,40] and taking into account the experimental feasibility, the optimal structural parameters of the PGMR filter with targeted wavelength of 606 nm can be obtained as follows: d_{cap} = 200 nm, d_g = 240 nm, d_w = 180 nm, F = 0.4, and Λ = 400 nm. As can be seen from Fig. 1(b), two resonances exist when the channels are not filled with liquid. The one located around 530 nm is the guided mode supported by the capping layer, while the one around 606 nm is the guided mode in the PVK layer. Their corresponding electric field distributions within a unit cell are plotted in Fig. 1(c) and (d). Note that when the channels are filled with liquid, the guided mode in the capping layer disappears since the effective index of the grating (n_{eff}) is close to the capping layer (n_{cap}). Thus our following study will focus on the guided mode in the PVK

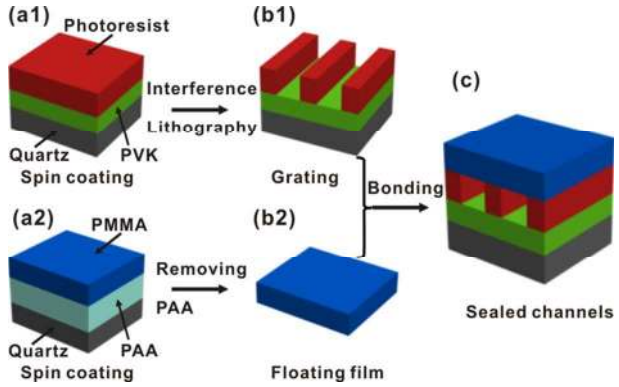

Fig. 2 Fabrication scheme of a single-layer polymer submicro-channel array. (a1) Spin-coating of a photoresist film on a poly(9-vinylcarbazole) (PVK) layer; (b1) Fabrication of a grating structure via interference lithography. (a2) Spin-coating of Poly (methyl methacrylate) (PMMA) film on a polyacrylic acid (PAA) layer; (b2) Preparation of a suspended PMMA film on the de-ionized water surface by removing sacrificial layer (PAA). (c) Bonding suspended PMMA film and grating layer together, a sealed submicro-channel array was formed.

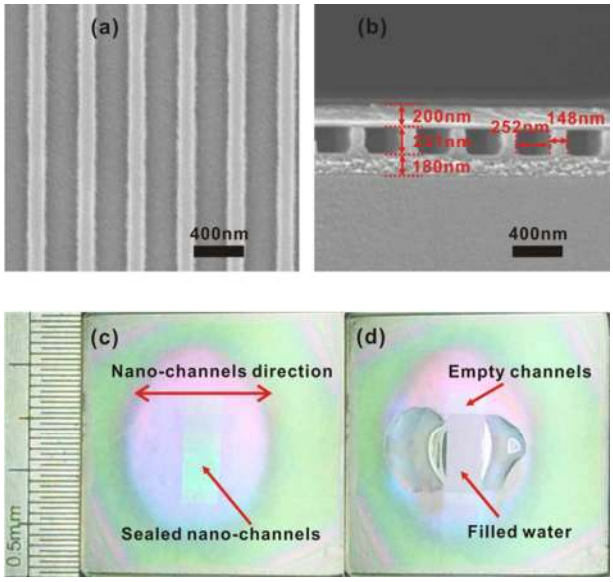

Fig. 3 (a) and (b) are SEM images of the top view of the grating and the cross-section view of the polymer submicro-channels with a 400 nm period. (c) and (d) are photographs of the fabricated submicro-optofluidic PGMR filter with empty channels and with water filled channels, respectively.

layer. The reflectance of the PGMR filter is almost 100% at the peak position around 606 nm, and is less than 2% in the off-resonance regime. The reflectance curve shows typical asymmetrical Fano line-shape due to the interference of the sharp guided mode resonance and the nonzero reflection background (the line-shape becomes more Lorentz-like when the antireflection condition of the multilayer is satisfied).[41]

To achieve a tunable submicro-optofluidic PGMR filter, liquids with various refractive indices can be injected into the submicro-channels. When the refractive index of liquids increases from 1.333 to 1.413, the reflection peak shifts towards longer wavelength for about 3.8 nm and the bandwidth of the peak becomes narrower, as shown in Fig. 1(b). The increased Q factor of the resonance is mainly due to the decreased scattering loss in the grating layer when the refractive index of liquid n_L gradually approaches n_H. As a result of the increased Q factor, more energy is confined into the waveguide layer, which can be seen from the increased peak value of the electric field amplitude, as shown in Fig. 1(e).

To demonstrate a tunable submicro-optofluidic PGMR filter, a novel nano-fabrication technology is developed, and the procedure is schematically shown in Fig. 2. Basically, there are three steps: forming grating structure, preparing floating PMMA film and bonding grating and floating film together. The detailed information is as follows.

For the fabrication of grating structure, a layer of poly(9-vinylcarbazole) (PVK, MW = 1,100,000, 3 wt% in chlorobenzene) was first spun onto a quartz substrate with a spin speed of 4000 r. p. m. for 32 s. Subsequently, the sample was baked on a hot plate at 180 ℃ for 10 minutes. The resulting thickness of the PVK film was about 180 nm. Then, a layer of positive photoresist (AR-P 3740, *AllResist*) with a thickness of 240 nm was spun on the PVK film at 4,000 r. p. m. for 32 s from a 10 wt% solution in a thinner (AR 300-12, *AllResist*). The photoresist was baked on a hotplate at 95℃ for 90 s. The photoresist was exposed to an interference pattern produced by two continuous coherent laser beams (457.9 nm).[42-44] After the exposure, the photoresist was developed by immersing in a solution of diluted developer AR 300-26 from AllResist (developer : de-ionized water = 1 : 4) at 22 ℃ for 25 s. The exposed region of photoresist was dissolved while the unexposed region remains, a grating structure was formed as shown in Fig. 2(b1).

For the preparation of a floating film, a thin sacrificial layer was first spun onto a clean quartz substrate at 4000 r. p. m. for 32 s with a solution of 2 wt% polyacrylic acid (PAA, MW = 1800) in ethanol, and baked on a hot plate at 115 ℃ for 5 minutes. The resulting thickness of the PAA layer was about 200 nm. After that, the Poly (methyl methacrylate) (PMMA, Mw = 350,000) film as a capping layer was spun onto the PAA film with a 3 wt% solution in chlorobenzene at 4000 r. p. m. for 32 s. The sample was then baked on a hot plate at 180 ℃ for 5 minutes. The thickness of the PMMA film was about 200 nm. Thereafter, the sample was immersed in de-ionized water, and a floating PMMA film was formed after the PAA layer was dissolved in water, as shown in Fig. 2(b2).

Finally, we bonded the floating PMMA film and grating structure together. To transfer a layer of floating PMMA film onto a hydrophobic polymer substrate, oxygen plasma treatment is required; otherwise the transferred PMMA layer will show lots of wrinkles. Moreover, plasma modification can be used for reducing processing temperatures and improving bonding strength for microfluidic chips.[45,46] The patterned photoresist film from previous step was first exposed to oxygen plasma at an oxygen flow rate of 600 sccm and a voltage of 500 V for 30 s. Subsequently, a floating PMMA film in de-ionized water was transferred and attached onto the patterned photoresist film, and the sample was dried in an ambient temperature. We then employed thermal bonding method to bond the photoresist and PMMA together at 105 ℃ just near their glass transition temperature for 2 minutes, an array of sealed polymer

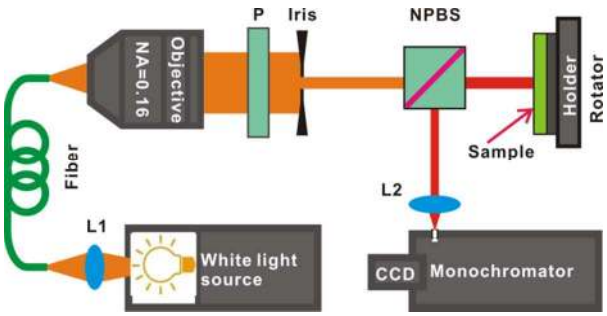

Fig. 4 Schematic setup for the reflection measurement. L1 and L2 are lenses that are used to collect and focus the light, P: a polarizer is used to select the polarization state of the incident light, NPBS: a non-polarizing beam splitter is used to separate the reflection response from the incident light.

submicro-channels was formed as shown in Fig. 2(c). Compared with the previous reported tunable GMR filters[14-20] which were fabricated by nano-replica or standard semiconductor nanofabrication method, our method is cost-effective and cheap, because it doesn't require a mask or complicated and expensive facilities. Furthermore, it is easy to form a sealed polymer submicro-channel array.

The top view of the grating and cross-section view of the sealed submicro-channels on a quartz substrate are shown in Fig. 3(a) and 3(b), respectively. The grating edge and surface are smooth, indicating good fabrication quality with interference lithography. As shown in Fig. 3(b), PVK waveguide layer, photoresist grating, and PMMA capping layer are clear from bottom to top. The thicknesses of the PVK, grating and PMMA layers are about 180, 231, and 200 nm, respectively. The thickness is slightly deviated from the designed values due to the fabrication errors. The period of the grating is 400 nm as designed; the width of grating ridge is about 148 nm, while the width of the channel is around 252 nm. Although the thermal bonding temperature is close to the glass transition temperature of the photoresist, no deformation occurs. The cross-section of the PVK looks quite rough; this is caused by the aggregation of the gold nanoparticles during the evaporation of the conductive layer of gold for observing in SEM (see Supplementary Fig. S1).

Fig. 3(c) and Fig. 3(d) show the photos of a submicro-optofluidic PGMR filter without and with water in channels, respectively. The photos were taken by a camera without the assistance of a microscope. The elliptical pattern is the exposed regime (~ 18.5 mm × 13.5 mm) and the direction of the submicro-channels is along the minor axis of the ellipse. In order to fill the water into the submicro-channels easily, the size of the capping film is cut to 3.5 × 10.5 mm with a scalpel. To further confirm the bonding quality, de-ionized water is injected from one side of the submicro-channels, and the channels are filled spontaneously with water due to capillary force. By comparing Fig. 3(d) with Fig. 3(c), we can see that the color of the sealed region changes once the empty channels are filled with water.

To confirm the tunability of our submicro-optofluidic PGMR filter, the reflection spectra of the fabricated device were measured by using a spectrum analyzer. A schematic setup for the optical reflection measurement at normal incidence is shown in Fig. 4. we used a halogen lamp as a white light source, from

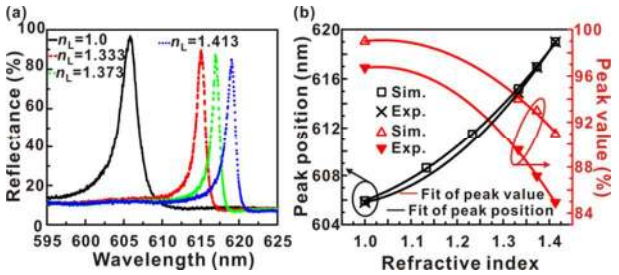

Fig. 5 (a) Experimental reflectance spectra of a tunable submicro-optofluidic PGMR filter. The black solid, red dashed , green dotted, and blue dotted curves indicate the reflectance spectra of the submicro-optofluidic PGMR filters with their submicro-channels filled with air, water, 32 wt% glycerine in water, and 60 wt% glycerine in water respectively, the corresponding refractive indices are 1.0, 1.333, 1373, 1413. (b) The dependence of resonant wavelength and peak value on the refractive index.

which the white light was collected and coupled into a multi-mode optical fiber by a lens with a focal length of 100 mm. The output light from the exit of the optical fiber was collimated by an objective lens with a numerical aperture value of 0.16. A polarizer was mounted in front of an iris, and the iris was used to yield a beam with a diameter of 0.5 mm. It should be noted that we only measured the reflectance of the sample when the polarization of the incident light is parallel to the grating ridges. A non- polarizing beam splitter was placed in the optical path to separate the reflection response from the incident light. Like most guided-mode resonance filters,[21,47,48] the spectral profile and the reflection peak position of the PGMR filter are also very sensitive to the angle of incidence. Hence, a rotatable sample holder was used to fine tune the angle of the sample so that the incident light can be perpendicular to the sample surface. The reflection light from the sample was collected and coupled into a spectrometer with a wavelength resolution of 0.02 nm by a lens with a focal length of 80 mm. The zeroth order reflection spectra were analyzed using a spectrometer of Acton SP2750 with a liquid-nitrogen-cooled CCD (SPEC-10, Princeton) power detector.

We measured the reflectance of the submicro-fluidic PGMR filter when the submicro-channels were not filled with any solutions, as shown by the black solid curve in Fig. 5(a). The corresponding simulation results are shown in Fig. 1(a). The measured reflection peak position is at 605.817 nm, whereas the simulated one is at 605.927 nm, as shown in Fig. 5(b). The small deviation of the peak position is mainly due to the fabrication errors. The measured reflectance at the side band is higher than the simulated one, which is caused by the additional reflection (~ 3.4%) from the backside of the quartz substrate that was not considered in the simulation. This problem can be overcome by depositing antireflection coating on the back side.

To further show the tunability of the PGMR filter, we measured the reflection spectra of the PGMR filter when the channels were filled with a series of mixture of glycerine and water. The concentrations of glycerine in water were chosen to be 0, 32%, and 60% in weight, and the corresponding refractive indices were 1.333, 1.373, and 1.413, respectively. The measured reflectance spectra are plotted in Fig. 5(a) by red dashed, green dotted and blue dotted curves, respectively. The resonance peak position versus the refractive index is further highlighted in

Table 1 Summary of different tunable GMR filters in the visible region

Architecture	Structure materials	Tuning mechanism	Tuning range (nm)	References
2-layer	TiO_2, UV-cured polymer	Optically tuned	25.39	19
2-layer	TiO_2, UV-cured polymer	Electric-optic effect	2.5	15
2-layer	TiO_2, PDMS	MEMS	17.6	20
3-layer	Si_3N_4, Gold	Index modulation	13.6	13
3-layer (sim.)	PMMA, PVK Photoresist	Optofluidics	13.071	Present work
3-layer (exp.)	PMMA, PVK, photoresist	Optofluidics	13.181	Present work

Fig. 5(b). The reflection peak wavelength red shifts from 605.817 nm to 618.998 nm in response to the change of refractive index from 1.0 to 1.413.The experimental tuning band width is 13.181 nm, which is comparable to the previous reported results shown in Table 1. Meanwhile, the full width at half maximum (FWHM) of the reflectance peaks reduces from 2.504 nm to 1.090 nm due to reduced scattering loss mentioned above, but the peak value of reflectance is still reasonably high (> 85%) over the broad tuning regime. The experimental data is in good agreement with the simulation results, as shown in Fig. 5 (b). It should be noted that all optical experiments were operated at the temperature of 22 ^oC. If it is considered the thermal effect, assuming that the refractive index change of all materials per temperature is 10^{-4}, the shift of the reflection peak is about 0.3 nm when the temperature changes from 20 ^oC to 30 ^oC. This shift is still negligible compared to the narrowest band width (1.090 nm) of the peak. Our study shows that the idea of using submicro-optofluidics as a novel mechanism to fine tune the response of polymer-based GMR filter is feasible and practical.

In conclusion, we theoretically proposed and experimentally demonstrated a reconfigurable polymer guided-mode resonance (PGMR) filter based on nano/microfluidic tuning. The submicro-optofluidic PGMR filter was fabricated by combining two beam interference lithography, floating nanofilm transfer, and thermal bonding technology. We demonstrated the tunability of the device by filling various fluids with different refractive index into the submicro-channels. The submicro-optofluidic PGMR filter has a tuning range of 13.181 nm, with a tuning efficiency of 49.31 nm/RIU, and a high reflection efficiency (> 85%) in the visible wavelength. The experimental data are in good agreement with the simulation results. Such a tunable submicro-optofluidic PGMR filter has potential applications in various lab-on-a-chip systems.

Acknowledgements

The authors acknowledge the financial support from the National Natural Science Foundation of China (11374376, 11174374, 11104359), the Key project of DEGP (2012CXZD0001), and Innovative Talents Training Program for Doctoral Students of Sun Yat-sen University.

Notes and references

[a] *State Key laboratory of optoelectronic materials and technologies, School of Physics and Engineering, Sun Yat-Sen University, Guangzhou, 510275, China. Fax: +862084112282; Tel: +862084112282; E-mail: jinchjun@mail.sysu.edu.cn*
[b] *Nonlinear Physics Center, Research School of Physics and Engineering, Australian National University, Canberra, ACT 2601, Australia.*
[c] *Physics Department, Lancaster University, Lancaster LA1 4YB, UK*

† Electronic Supplementary information (ESI) available: The aggregation of the gold nanoparticles during the evaporation of the conductive layer of gold. See DOI: 10.1039/b000000x/

1 A. Hessel and A. A. Oliner, *Appl. Opt.* , 1965, **4**, 1275.
2 R. Magnusson and S. S. Wang, *Appl. Phys. Lett.* , 1992, **61**, 1022.
3 R. R. Boye, R. W. Ziolkowski and R. K. Kostuk, *Appl. Opt.* , 1999, **38**, 5181.
4 A. Sharon, D. Rosenblatt, A. A. Friesem, H. G. Weber, H. Engel and R. Steingrueber, *Opt. Lett.* , 1996, **21**, 1564.
5 T. Katchalski, G. Levy-Yurista, A. A. Friesem, G. Martin, R. Hierle and J. Zyss, *Opt. Express*, 2005, **13**, 4645.
6 D. W. Peters, R. R. Boye, J. R. Wendt, R. A. Kellogg, S. A. Kemme, T. R. Carter and S. Samora, *Opt. Lett.* , 2010, **35**, 3201.
7 X. Buet, E. Daran, D. Belharet, F. Lozes-Dupuy, A. Monmayrant and O. Gauthier-Lafaye, *Opt. Express*, 2012, **20**, 9322.
8 G. Niederer, H. P. Herzig, J. Shamir, H. Thiele, M. Schnieper and C. Zschokke, *Appl. Opt.* , 2004, **43**, 1683.
9 M. J. Uddin and R. Magnusson, *IEEE Photon. Technol. Lett.* , 2012, **24**, 1552.
10 C. Y. Yang, L. Hong, W. D. Shen, Y. G. Zhang, X. Liu and H. Y. Zhen, *Opt. Express*, 2013, **21**, 9315.
11 K. H. Jia, D. W. Zhang and J. S. Ma, *Sens. Actuators, B*, 2011, **156**, 194.
12 X. Wei and S. M. Weiss, *Opt. Express*, 2011, **19**, 11330.
13 S. Lin, C. Wang, T. Ding, Y. Tsai, T. Yang, W. Chen and J. Chang, *Opt. Express*, 2012, **20**, 14584.
14 A. S. P. Chang, K. J. Morton, H. Tan, P. F. Murphy, W. Wu and S. Y. Chou, *IEEE Photon. Technol. Lett.* , 2007, **19**, 1457.
15 F. Yang, G. Yen and B. T. Cunningham, *Appl. Phys. Lett.* , 2007, **90**, 261109.
16 A. D'alessandro, D. Donisi, L. De Sio, R. Beccherelli, R. Asquini, R. Caputo and C. Umeton, *Opt. Express*, 2008, **16**, 9254.
17 M. J. Uddin and R. Magnusson, *IEEE Photon. Technol. Lett.* , 2013, **25**, 1412.
18 D. W. Dobbs and B. T. Cunningham, *Appl. Opt.* , 2006, **45**, 7286.
19 F. Yang, G. Yen, G. Rasigade, J. A. N. T. Soares and B. T. Cunningham, *Appl. Phys. Lett.* , 2008, **92**, 091115.
20 S. Foland, B. Swedlove, H. Nguyen and J. B. Lee, *J. Microelectromech. Syst.* , 2012, **21**, 1117.
21 Z. S. Liu, S. Tibuleac, D. Shin, P. P. Young and R. Magnusson, *Opt. Lett.* , 1998, **23**, 1556.
22 C. G. Chen, X. W. Zhang, J. B. Zhu, J. Li, L. B. Zhang and E. Wang, *Nanoscale*, 2013, **5**, 8221.
23 J. Heo, H. J. Kwon, H. Jeon, B. Kim, S. J. Kim and G. Lim, *Nanoscale*, 2014, **6**, 9681.
24 D. Psaltis, S. R. Quake and C. Yang, *Nature*, 2006, **442**, 381.
25 Z. G. Li, Y. Yang, X. M. Zhang, A. Q. Liu, J. B. Zhang, L. Cheng and Z. H. Li, *Biomicrofluidics*, 2010, **4**, 043013.
26 Z. Yu, R. S. Liang, P. X. Chen, Q. D. Huang, T. T. Huang and X. K. Xu, *Plasmonics*, 2012, **7**, 603.
27 A. S. Jugessur, J. Dou and J. S. Aitchison, *J. Vac. Sci. Technol. B*, 2010, **28**, C6O8.
28 Y. C. Seow, S. P. Lim and H. P. Lee, *Appl. Phys. Lett.* , 2009, **95**, 114105.
29 W. Z. Song and D. Psaltis, *Lab Chip*, 2013, **13**, 2708.
30 Y. Yang, A. Q. Liu, L. Lei, L. K. Chin, C. D. Ohl, Q. J. Wang and H. S. Yoon, *Lab Chip*, 2011, **11**, 3182.
31 L. K. Chin, A. Q. Liu, C. S. Lim, C. L. Lin, T. C. Ayi and P. H. Yap, *Biomicrofluidics*, 2010, **4**, 024107.
32 W. Zhang, H. Zappe and A. Seifert, *Light: Sci. Appl.* , 2014, **3**, e145.
33 X. G. Tang, R. J. Li, J. K. Liao, H. P. Li, J. F. Li and Y. Liu, *Opt. Commun.* , 2013, **305**, 175.

34 L. K. Chin, A. Q. Liu, Y. C. Soh, C. S. Lim and C. L. Lin, *Lab Chip*, 2010, **10**, 1072.
35 A. S. Jugessur, J. Dou, J. S. Aitchison, R. M. De La Rue and M. Gnan, *Microelectron. Eng.* , 2009, **86**, 1488.
36 Y. B. Guo, H. Li, K. Reddy, H. S. Shelar, V. R. Nittoor and X. D. Fan, *Appl. Phys. Lett.* , 2011, **98**, 041104.
37 W. X. Liu, Z. Q. Lai, H. Guo and Y. Liu, *Opt. Lett.* , 2010, **35**, 865.
38 S. S. Wang and R. Magnusson, *Appl. Opt.* , 1993, **32**, 2606.
39 D. Shin, S. Tibuleac, T. A. Maldonado and R. Magnusson, *Opt. Eng.* , 1998, **37**, 2634.
40 J. N. Liu, M. V. Schulmerich, R. Bhargava and B. T. Cunningham, *Opt. Express*, 2011, **19**, 24182.
41 S. Tibuleac and R. Magnusson, *J. Opt. Soc. Am. A*, 1997, **14**, 1617.
42 Y. Shen, J. H. Zhou, T. R. Liu, Y. T. Tao, R. B. Jiang, M. X. Liu, G. H. Xiao, J. H. Zhu, Z. K. Zhou, X. H. Wang, C. J. Jin and J. F. Wang, *Nat. Commun.* , 2013, **4**, 2381.
43 T. R. Liu, Y. Shen, W. Shin, Q. Z. Zhu, S. H. Fan and C. J. Jin, *Nano Lett.* , 2014, **14**, 3848.
44 Q. Z. Zhu, S. P. Zheng, S. J. Lin, T. R. Liu and C. J. Jin, *Nanoscale*, 2014, **6**, 7237.
45 M. E. Vlachopoulou, A. Tserepi, P. Pavli, P. Argitis, M. Sanopoulou and K. Misiakos, *J. Micromech. Microeng.* , 2009, **19**, 015007.
46 Y. H. Tennico, M. T. Koesdjojo, S. Kondo, D. T. Mandrell and V. T. Remcho, *Sens. Actuator, B*, 2010, **143**, 799.
47 G. Niederer, W. Nakagawa, H. P. Herzig and H. Thiele, *Opt. Express*, 2005, **13**, 2196.
48 A. Szeghalmi, M. Helgert, R. Brunner, F. Heyroth, U. GÖSele and M. Knez, *Adv. Funct. Mater.* , 2010, **20**, 2053.